Statistical Wound-Rotor IM Diagnosis Method Based on Standard Deviation using NVSA

Khalid Dahi, Soumia Elhani and Said Guedira

***Abstract*—** In this paper we address the problem of rotor faults in Wound Rotor Induction Machine by using two different signal processing methods to voltage between neutrals such as Standard deviation calculation and Hilbert Transform (HT). This last is employed as an effective technique for fault detection in induction machines. The mathematical simplicity of the proposed technique, compared with some commonly used algorithms from the literature, renders it competitive candidate for the on-line diagnosis of machines.

Experimental results are provided to verify the proposed method and to evaluate its performance as pre-processing for monitoring of Wound Rotor Induction Machine. An algorithm has been tested on neutral between voltages under different load conditions and rotor fault degrees that shows that the studied diagnosis method can be used as a valid methodology for this type of phenomena.

***Keywords*—** Diagnosis; Rotor fault; WRIM; Neutral voltage; Standard deviation.

I. Introduction

WOUND Rotor Induction Machine WRIM has recently known a new life due to the worldwide development, The wound rotor induction machine offers a number of advantages over other types of asynchronous machines, including the ability to produce a high starting torque with low starting current, and also they are easy assembly compared to asynchronous squirrel cage machine, thanks to these benefits that the WRIM is frequently used in the industry for any application requiring large rotating machines. However, these wind generators suffer from some electric stresses that can affected the profitability of these machines.

In this type of application, monitoring of WRIM is crucial due to their working environment, and fault diagnostics requires measures sensitive to the change greatness of the WRIM and an appropriate method to obtain a diagnostic index and a threshold indicating the limit between the healthy state and the defective one. There are a number of research papers on technical monitoring of electrical machines which are most relevant are [1] - [6].

K.Dahi and S.Elhani are with the Department of electrical engineering, at the Ecole Normale Supérieure de l'Enseignement Technique, Mohammed V Souissi University, Rabat-Morocco
(e-mail: Khalid.dahi@ um5s.net.ma; s.elhani@um5s.net.ma).

S. Guedira is with the "Ecole Nationale de l'Industrie Minérale" Rabat, Morocco, laboratoire de recherché commande protection et surveillance des installations industriels (e-mail: said.guedira@gmail.com).

Studies carried out by articles have shown that defects of the stator windings and rotor windings are assumed equal because they are inadequately protected. However, the vast majority of articles dealing mainly with rotor fault first and then with stator faults and finally bearing faults.

In this paper we focus on the rotor fault, this fault which physically resembles to the stator fault resulting either by short/open circuits or by increasing of the rotor resistance. In this case, the machine can also operate after the application of a fault, while in case of short/open circuits the machine operation is limited by a brief duration. In our case an additional resistance is added to one of the phases of the rotor to create the rotor fault.

Generally, MCSA "Motor Current Signal Analysis" [7] [8] [9][10]. (Widely known in the literature) is the most commonly used technique and well established. In fact, MCSA is simple and effective in appropriate operating conditions. However, this technique has significant limitations due to the increasing complexity of electrical machines and drives [1]:

1) It is influenced by the operating conditions (e.g. low load conditions, load oscillations);
2) The fault diagnosis is difficult or impossible if the system operates under time-varying conditions or the machine is supplied by a power converter;
3) The diagnosis is difficult or impossible in machines with special magnetic structure (e.g. machines with double cage in which there are a strong influence of interbar currents or only the outer cage has a fault).
4) The induction machines are now frequently installed with inverters which provide a number of advantages and therefore make the stator current inaccessible to diagnosis.

To reduce these limitations, the proposed work focuses on the use of voltage between neutrals NV "Neutral Voltage" [12] - [17] that we will name in this paper V_{NN}. The method has performance comparable to MCSA or better is based on the analysis of the potential difference between the neutral of star-connected stator and the neutral network in the case of a direct feed or artificial neutral in the case of a supply voltage by inverter in order to detect a rotor fault in induction machine.

In addition, by using this signal we follow the same steps as G.DIDIER [9] who has developed a method by MCSA for the detection of rotor faults without need to reference, this reference obtained in a healthy functioning. This approach is based on standard deviation calculations taken on two

frequency ranges, the first standard deviation will be calculated on the first frequency range, this range identifies where the phase jump whose frequency (*3-4s*)*fs*. The second standard deviation is a picture of measurement noise present between jumps being located at frequencies (*3-4s*)*fs* and (*3-6s*)f_s.

Thereafter, an analysis of phase spectra by the Hilbert transform is made, this transform is usually used in image processing, where the phase contains more relevant information than its module, its advantage is that the Hilbert transform calculated from the amplitude spectrum of the signal to analyze, which allows to conclude on the nature of fault.

This paper is organized as follows. Section II presents the theory background that we use in this study. The neutral voltage signal analysis NVSA is described in Section III. Proposed method is presented and explained in Section IV. In Section V, experimental results are validated and discussed.

II. Theory Background

The purpose of this section is to present some mathematical signal processing notions used to develop the studied method. To permit the reader to navigate the various strands, this section is subdivided into three main topics: Fourier and Hilbert transform, discrete Hilbert transform and standard deviation.

A. Phase Fourier transform

Recall the mathematical equation of the Fourier transform of a finite sequence ***{ps (0). . . , P (N - 1)}***

$$\mathcal{F}(k)=\frac{1}{N}\sum_{n=0}^{N-1}p_s(n)e^{-j\frac{2\pi nk}{N}} \tag{1}$$

By applying this relationship, the result is a complex signal with a real part and an imaginary part such as:

$$\mathcal{F}(k)=\Re(\mathcal{F}(k))+j\Im(\mathcal{F}(k)) \tag{2}$$

In our work we are interested in the form of the phase of NV, the phase of the Fourier transform is given by:

$$\varphi_{FT}(k)=\arctan\left(\frac{\mathcal{F}_{\mathrm{Im}(k)}}{\mathcal{F}_{\mathrm{Re}(k)}}\right) \tag{3}$$

B. Hilbert Transform

To start we present first the theory of the Hilbert transform

Let's consider a real measurement signal: $x(t)\in\mathcal{L}^{(2)}$

Where $L^{(2)}$ is the signal class with integral square

The Hilbert transform of the signal *x*(*t*) is : [18][19]

$$\tilde{x}(t)=\mathcal{H}\{x(t)\}=\int_{-\infty}^{\infty}\frac{x(\tau)}{\pi(t-\tau)}d\tau \tag{4}$$

$\tilde{x}(t)$ is improper named the conjugate of *x*(*t*), and we also have : $\tilde{x}(t)\in\mathcal{L}^{(2)}$

x(*t*) is the inverse Hilbert transform of $\tilde{x}(t)$

$$x(t)=\mathcal{H}^{-1}\{\tilde{x}(t)\}=-\frac{1}{\pi}\int_{-\infty}^{\infty}\frac{\tilde{x}(t)}{t-\tau}d\tau \tag{5}$$

Let's observe that $\tilde{x}(t)$ is determined by the convolution of *x*(*t*) with the signal 1/πt:

$$\tilde{x}(t)=x(t)*\frac{1}{\pi t} \tag{6}$$

Like Fourier transforms, Hilbert transforms are linear operators.

The above relation allows the calculus of the spectral density of $\tilde{x}(t)$:

$$\tilde{X}(j\omega)=X(j\omega).\mathcal{F}\{\frac{1}{\pi t}\} \tag{7}$$

Since: $$\mathcal{F}\left\{\frac{1}{\pi t}\right\}=-j\,\mathrm{sgn}(\omega)$$

It results: $$\tilde{X}(j\omega)=X(j\omega)\left[-j\,\mathrm{sgn}(\omega)\right] \tag{8}$$

Or:

$$\tilde{X}(j\omega)=\begin{cases}-jX(j\omega),\omega>0\\ jX(j\omega),\omega<0\end{cases} \tag{9}$$

As a result, the spectral density function of the *x*(*t*) signal's conjugate is obtained by changing the phase of the spectral density for *X*(*jω*) by ±π/2. And it results:

$$\tilde{x}(t)=\mathcal{H}\{x(t)\}=\mathcal{F}^{-1}\{\tilde{X}(j\omega)\} \tag{10}$$

Taking into account relation (8) it results:

$$x(t)=-\mathcal{H}\{\tilde{x}(t)\}=\begin{cases}-\mathcal{F}^{-1}\{j\tilde{X}(j\omega)\},\omega>0\\ \mathcal{F}^{-1}\{-j\tilde{X}(j\omega)\},\omega<0\end{cases} \tag{11}$$

The analytic signal

A useful point of view to understand and to compute the Hilbert Transform of *x*(*t*) is using the analytic signal *z*(*t*) associated with *x*(*t*), defined, as explained before, as:

$$z(t)=x(t)+j\tilde{x}(t) \tag{12}$$

That can be rewritten also as:

$$z(t)=A(t)*e^{j\theta(t)} \tag{13}$$

Where *A*(*t*) is called the envelope signal of *x*(*t*) and *θ*(*t*) is called the instantaneous phase signal of *x*(*t*). In terms of *x*(*t*) and $\tilde{x}(t)$, it is clear that:

The use of Hilbert phase analysis is applied to the module of Fourier transformation frequency of the signal *x*(*t*). Indeed, the analytic signal and the corresponding phase are given by:

$$A(t)=[x^2(t)+\tilde{x}(t)]^{1/2} \tag{14}$$

$$\varphi(t)=\tan^{-1}\left[\frac{\tilde{x}(t)}{x(t)}\right]=2\pi f_0 t \tag{15}$$

Or:

$$\varphi(f)=\arctan\frac{\mathcal{H}\left[|X(f)|\right]}{|X(f)|} \tag{16}$$

And the "instantaneous frequency" is given by:

$$f_0=\left(\frac{1}{2\pi}\right)\tan^{-1}\left[\frac{\tilde{x}(t)}{x(t)}\right] \tag{17}$$

ISBN: 978-1-61804-243-9

C. Discrete Hilbert Transform

Having the signal $x(t)$ defined on the time interval $[0,t_N]$ using a sampling period T_e, we obtain the discrete signal $x[n]$:

$$x(n) = x(nT_e), n \in \overline{0, N-1} \tag{18}$$

Where: $T_e=t_N/N$

The sampling frequency f_e is chosen so that the frequency $f_e/2$ is greater or equal to the least significant frequency from the spectrum of $x(t)$. We consider the discrete frequency step:

$$f_0 = \frac{f_e}{N} \quad , \qquad \omega_0 = \frac{2\pi}{N} f_e \tag{19}$$

The discrete Fourier transform (DFT) is:

$$TFD\{x[n]\} = X[k] = \sum_{n=0}^{N-1} x[n] e^{-jnk\frac{2\pi}{N}}, k \in \overline{0, N-1} \tag{20}$$

The sample of the spectral density corresponding to frequency $k\omega_0$ is determined with the relation:

$$X(jk\omega_0) = T_e X[k] \tag{21}$$

Where $X(j\omega)$ is the Fourier transform in continuous time.

O the other hand:

$$X[k]^* = X[N-k] = X[-k] \tag{22}$$

Which show that the sample $X[N-k]=X[-k]$ has a correspondent sample of the spectral density, with the negative frequency $X(-k\omega_0)$.

Similarly to (10) the discrete Hilbert transform is defined as:

$$\mathcal{H}\{x[n]\} = \tilde{x}[n] = TFD^{-1}\{\tilde{X}[k]\} \tag{23}$$

Where for N-even:

$$\tilde{X}[k] = \begin{cases} -jX[k], k = 1, \overline{\frac{N}{2}-1}, Neven \\ jX[k], k = \overline{\frac{N}{2}+1, N-1}, Neven \end{cases} \tag{24}$$

D. Standard deviation formula:

The RMS can be computed in the frequency domain, using Parseval's theorem. For a sampled signal

$$\sum_n x^2(t) = \frac{\sum_n |X(f)|^2}{n} \tag{25}$$

Where $X(f)=\text{FFT}\{x(t)\}$ and n is number of $x(t)$ samples.

In this case, the RMS computed in the time domain is the same as in the frequency domain:

$$RMS = \sqrt{\frac{1}{n}\sum_n x^2(t)} = \sqrt{\frac{1}{n^2}\sum_n |X(f)|^2} \tag{26}$$

If is the arithmetic mean and is the standard deviation of a waveform then:

$$x_{rms}^2 = \tilde{x}^2 + \sigma_x^2 \tag{27}$$

The standard deviation (represented by the Greek letter sigma, σ) shows how much variation or dispersion from the average exists, and it's defined by:

$$\sigma_x = \sqrt{\frac{1}{N-1}\sum_{i=1}^{N}\left(x_i - \frac{1}{N}\sum_{i=1}^{N} x_i\right)^2} \tag{28}$$

III. Neutral Voltage Signal Analysis (NVSA)

A. NVSA frequency

1998, M.A.Cash [12] used the voltage between the neutral of the supply voltage and the neutral of induction machines (Fig. 1) to detect short circuits between spiral in stator coils. A similar analysis was carried out by [14] [15] in order to detect rotor fault in induction machines.

The voltage between the neutral and the neutral WRIM of the power source is given by the following mathematical relationship:

$$V_{NN} = R_a I_{sa} + L_a \cdot \frac{dI_{sa}}{dt} + \frac{dL_a}{d\theta}\Omega I_{sa} - V_{Supply} \tag{29}$$

Where:

R_a represents the stator-phase resistance,
L_a his inductance,
I_{sa} the current passing through it,
Ω Rotation speed, θ the angular position of the rotor and V_{supply} simple voltage generated by network supply.

The presence of a fault rotor reveals additional components in the spectrum of NV. Indeed, M.E.K. OUMAMMAR [17] demonstrated by a complex analysis, that the appearance of a rotor fault induces additional components in the frequency spectrum of the NV at frequencies given by the relation:

$$f_h = \lfloor 3h - (3h \pm 1)s \rfloor f_s \tag{30}$$

s: slip, f_s: supply frequency, h = 1,3,5, ...

The speed ripple induced additional harmonic components around the previous frequency, and the frequencies of all components can be expressed as follows:

$$f_h = \lfloor 3h(1-s) \pm s(1+2k) \rfloor f_s \tag{31}$$

B. FFT Analysis

The information given by the spectrum of the voltage at the third harmonic [11], i.e., nears the spectral line having the frequency 150 Hz can be used for WRIM fault diagnosis. We present in Fig.3 the power spectral density of NV for a rotor fault near this harmonic. We note the presence of the main frequency component (2) and additional components around these main components.

It is important to note that the rotor fault is created by adding an extra resistance on one of the rotor phase in order to have a dissymmetry in the rotor. For that the value of the rotor resistance has been progressively varied during the experiment from $R_{add} = 0$ to $R_{add} = 1.25R_r$, from this variation we can see its effect on the spectrum of the NV according to (27), the value of f_{fault} = 145 Hz.

In fig.2 is shown that the magnitude of the characteristic harmonic frequency due to a rotor fault changes as function of the additional resistance.

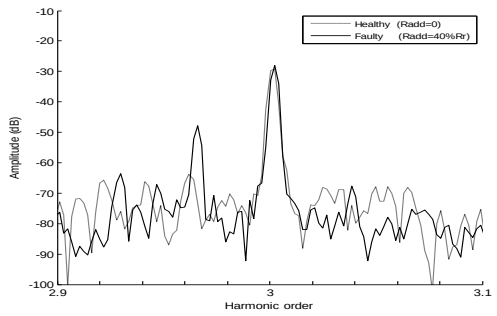

Fig. 1. Experimental results for the WRIM. Spectrum of neutral voltage in healthy (light black solid line) and faulty (solid line)

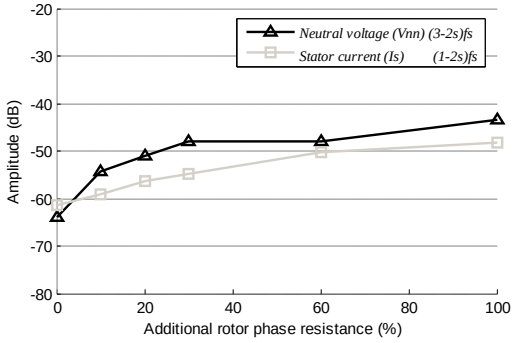

Fig. 2. Effect of a faulty operating conditions given by an increment of the rotor-phase resistance (neutral voltage and stator current)

IV. Proposed Method

In this work we perform a rotor fault diagnosis based on standard deviation calculation, for that we propose an algorithm to decision making by analyzing the exclusive NV signal.

Studies [15] [16] have shown that all asynchronous machines have a slight asymmetry of construction induced, in the spectrum of NV, a frequency component:

$$f_h = \lfloor 3h(1-s) \pm s(1+2k) \rfloor f_s \tag{32}$$

This method has been developed by G.DEDIER who used it on stator current analysis. We follow the same steps and we study first the phase $\varphi\mathcal{F}(f)$, particularly the jump present at the frequency $(3\text{-}4s)f_s$. Normally, this phase jump is very small or even zero for a healthy induction machine whatever the level of load. For the studied machine, figure 4 shows this slight fluctuation.

We propose the detection of a rotor fault by studying exclusively the phase jump located at the frequency $(3\text{-}4s)f_s$. We compare the standard deviation of the phase $\varphi\mathcal{H}(f)$ and the phase $\varphi\mathcal{F}(f)$ based on two different frequency ranges. Indeed, the first standard deviation, noted σ_j will be calculated on the frequency range (R_1), this range identifies where is the phase jump whose frequency $(3\text{-}4s)f_s$. The second standard deviation, which we note σ_n will be calculated on the frequency range (R_2) This standard deviation is a picture of measurement noise present between jumps being located at frequencies $(3\text{-}4s)f_s$ and $(3\text{-}6s)f_s$.

$$R_1 = \left\lfloor (3-4s) f_s - \frac{\delta}{2}, (3-4s) f_s + \frac{\delta}{2} \right\rfloor \tag{33}$$

$$R_2 = \left\lfloor (3-4s) f_s - \frac{\delta}{2}, (3-6s) f_s + \frac{\delta}{2} \right\rfloor \tag{34}$$

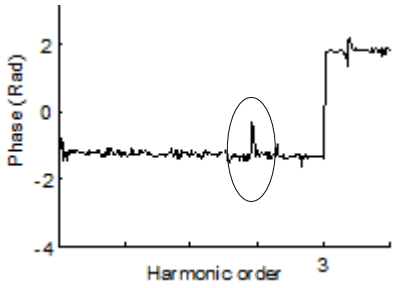

Fig. 3. Fluctuations at Spectrum phase in healthy case

The mathematical relationship to calculate the standard deviation σv, unbiased, of the Neutral Voltage is:

$$\sigma_v = \sqrt{\frac{1}{N-1}\sum_{i=1}^{N}\left(v_n - \frac{1}{N}\sum_{i=1}^{N} v_n\right)^2} \tag{35}$$

Fig. 5 shows a representation for an adequate understanding of the calculation of these deviations. The standard deviation σ_j is calculated on the gray frequency range while the standard deviation σ_n is calculated on the black frequency range.

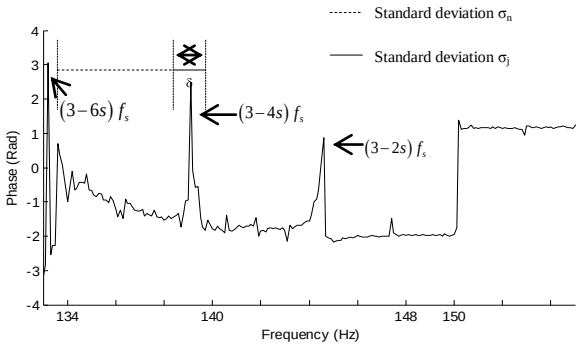

Fig. 4. Calculation of standard deviations σ_j and σ_n

For the further diagnosis it is necessary to calculate the slip s of the machine in both frequency ranges R_1 and R_2.

In most machines, the jump located at the frequency $(3\text{-}4s)f_s$ is always present in the Fourier and Hilbert phase, it adds that is this jump is more pronounced among other jumps (same thing for stator current phase, where $(1\text{-}2s)f_s$ is the most pronounced in the spectrum) .The calculation of this shift will inform us about the frequency $(3\text{-}4s)f_s$ desired. The detection of the jump located at the frequency $(3\text{-}2s)f_s$ is given since we know the fundamental frequency f_s.

The maximum slip of the machine allows obtaining the minimum frequency:

$$f_{def_{\min}} = (3 - 2s_{\max})\, f_s \quad (36)$$

The proposed methodology to diagnose rotor fault in WRIM is shown in Fig. 5 Based on these algorithm we present in the next section some experimental results to validate the proposed method.

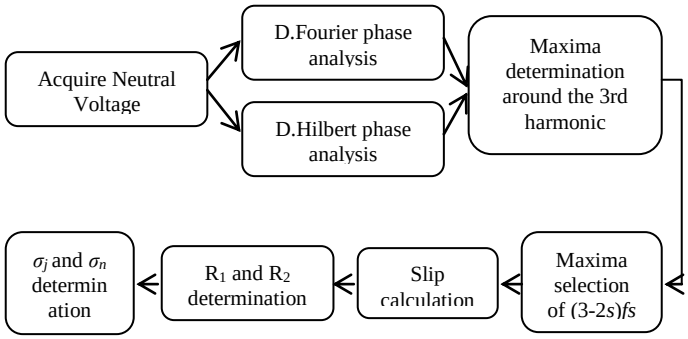

Fig. 5. Proposed methodology

V. Results and Discussion:

The diagnostic procedure presented in this paper has been tested through an off-line approach in which different degrees of additional resistance to create the rotor asymmetry have been forced in the WRIM.

A. Experimental Setup

Experimental Tests were developed on a 3kW, 50Hz, 220V/380V, 4-poles Wound Rotor Induction Machine (Table.IV and V). The motor was directly coupled direct current machine acting as a load. Two voltage sensors are used to monitor the induction machine operation. The IM voltages are measured by means of the two sensors which are used as inputs of the signal conditioning and the data acquisition board integrated into a personal computer.

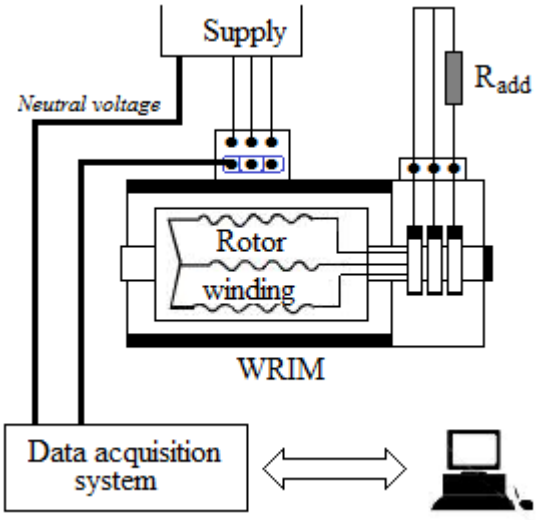

Fig. 6. Experimental set-up

For those two variables, the sampling frequency was 2 kHz and each data length was equal to 2^{14} values. Eight data sets of induction machines neutral voltage subject to different numbers of rotor fault and load conditions were analyzed (Table I).

TABLE I Analyzed Data sets

Set	Machine condition
s1	Healthy, unloaded
s2	Healthy, 75% Load
s3	Healthy, Full load
s4	Fault, unloaded
s5	Fault, 75 % load, R_{add}=10%R_r
s6	Fault, 75 % load, R_{add}=20%R_r
s7	Fault, 75 % load, R_{add}=100%R_r
s8	Fault, 100 % load, R_{add}=10%R_r

B. Method diagnosis based on Fourier transform phase analysis

In this section, we apply the detection method described above on NV when the machine is directly connected to the three-phase network.

The results are presented in Table II, the first column of this table corresponds to the rotor state, the second gives the value of the frequency $(3\text{-}2s)f_s$, third and fourth in succession values σ_j and σ_n calculated on the frequency ranges R_1 and R_2, the fifth gives σ_j/σ_n report that allows the decision making by the last column. Thus, we represent in Fig.6 curve $\varphi\mathcal{F}(f)$ phases for s2, s4,s5,s6,s7 and s8 tests.

According to the column giving σ_j/σ_n report we note that it is low for a machine operating with a healthy rotor, then we perceive that for some healthy functioning we do not detect jump phase $(3\text{-}2s)f_s$ in this case we consider the rotor in good condition.

The appearance of a partial rotor fault does not induce a significant increase of σ_j relative to σ_n, which does not allow to conclude on such a failure, it may be the low point method using $\varphi\mathcal{F}(f)$. For an important rotor fault (s8) we note that this report is greater 10 times that in tests where the machine is healthy

From the results of the Table II, we can validate the proposed approach, even if σ_j/σ_n report in tests s6 and s5 is less pronounced as seen in Table II, but the results are satisfactory.

According to Fig. 7 and Table II, the first problem for this approach is the high level of noise in the frequency range studied. The second problem is the wrong detection of the phase jump at frequencies located at frequency characterizing the rotor fault for the NVSA. In fact, the presence of random phase jumps in the frequency range does not allow proper detection of the phase jump required to calculate the slip.

ISBN: 978-1-61804-243-9

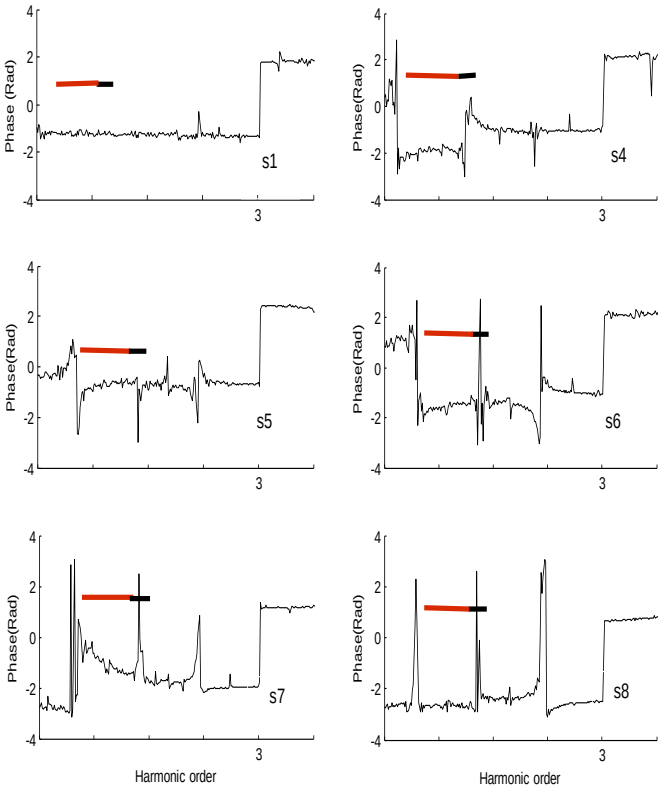

Fig. 7. Standard deviations σ_j and σ_n calculation by $\varphi F(f)$

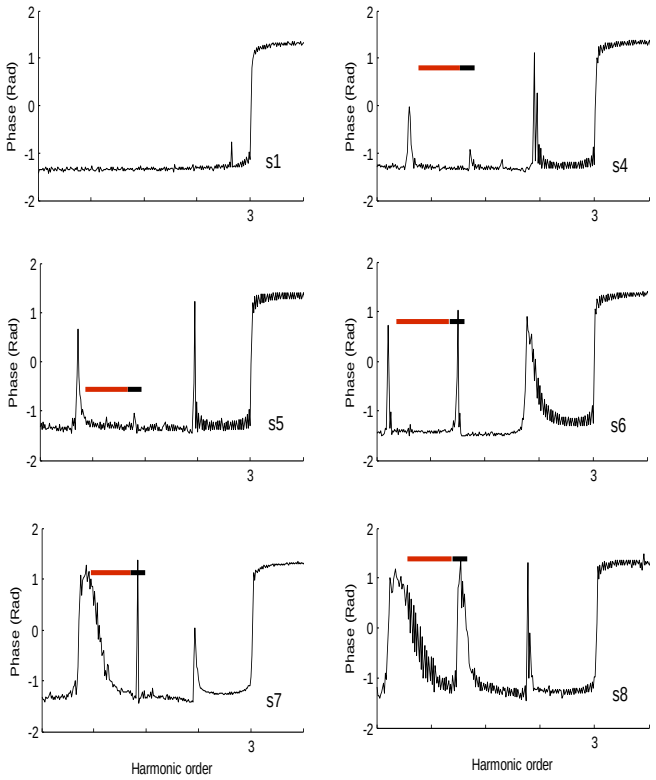

Fig. 8. Standard deviations σ_j and σ_n calculation by $\varphi \mathcal{H}(f)$

TABLE II RESULTS OF DIAGNOSTIC METHOD APPLIED TO THE PHASE OF THE FOURIER TRANSFORM

Rotor state	*(3-2s) fs.* (Hz)	*(3-4s) fs.* (Hz)	σ_n	σ_j	$\frac{\sigma_J}{\sigma_N}$
s1	No max detection				
s2	No max detection				
s3	145.23	139.19	0.240	0.091	2.64
s5	144.40	138.81	0.065	0.063	1.03
s8	146.33	140	0.969	0.026	37.30
s4	144.40	138.81	0.240	0.091	2.64
s6	143.8	138	0.51	0.079	6.52
s7	142.95	137.31	0.42	0.051	8.34

C. Hilbert transform phase analysis

We have already seen that even the good results that phase spectrum analysis compared to the module spectrum analysis, this method has two drawbacks.

1) The noise level is high, which makes detection difficult.
2) The second is that the form of the phase is not fixed. Indeed, the real and imaginary parts can take random values.

To stabilize the form of phase, we must find a solution to control the values of the real and imaginary parts of the spectrum, the idea is to obtain a phase always equal to$[-\pi/2]$ to the left of *f*s and equal to $[\pi/2]$ right f_s, the real part must be zero at frequencies $\pm f_{def}$ and f_s.

These problems can be circumvented with the use of the Hilbert transform, as we will see below.

In order to support the results obtained, we give in Fig. 8 the curves of phase $\varphi \mathcal{H}(f)$ with different fault level. In these figures, we stand once again by a continuous gray line the frequency range where the standard deviation σ_j is calculated, for a continuous black line the frequency range where the standard deviation σ_n is calculated, and a red line the maximum of the phase jump at the frequency located at $(3\text{-}2s)f_s$.

By use of the Hilbert transform (Table III), the two sets s4 and s5 were detected which is not the case when using the Fourier transform. Except this particular case, the results are better than those given in Table II. This better detection is possible because the noise in the phase of the signal analysis is much less important when the machine is running at low load torque. In addition, it is important to note that the signals obtained by the Hilbert transform are much less noisy than those calculated from the Fourier transform.

We show in Fig. 9 a comparison between the Hilbert approach and Fourier one in both healthy and faulty cases. We note that the σ_j/σ_n report does not vary too much despite the variation in the load level. In the defective case we see a notable variation between fault conditions.

From Fig.9, we note that the σ_j/σ_n report does not exceed 3 for a healthy machine and it is greater than 3 for a defective machine. This conclusion led the authors in [9] to operate to make an induction machine diagnosis method without reference (this reference usually obtained from a healthy functioning). In other words if the report σ_j/σ_n is less than 3

ISBN: 978-1-61804-243-9

then the machine is healthy, and defective if greater than 3.

From this result we can draw a law diagnostic decision support such as that given by G.DEDIER[9].

TABLE III RESULTS OF DIAGNOSTIC METHOD APPLIED TO THE PHASE OF THE HILBERT TRANSFORM

Rotor state	*(3-2s)fs* (Hz)	*(3-4s)fs* (Hz)	σ_n	σ_J	$\frac{\sigma_J}{\sigma_N}$
s1	No max detection				
s2	145.23	139.19	0.384	0.108	3.56
s3	145.23	139.19	0.105	0.073	1.45
s5	144.40	138.81	0.056	0.005	10.64
s8	146.33	140	0.29	0.003	79.30
s4	144.40	138.81	0.015	0.007	2.15
s6	143.8	138	0.302	0.006	48.01
s7	142.95	137.31	0.36	0.006 3	56.3

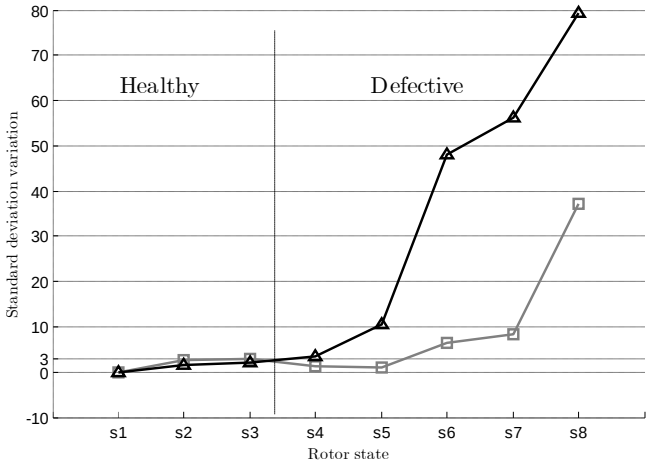

Fig. 9. Hilbert (Black line) and Fourier Transform (Gray line) method comparison

VI. Conclusion

Two approaches have been proposed to diagnose rotor fault. The first approach is based on the calculation of Fourier transform phase of Neutral Voltage. This phase contained relevant information on the status of the asynchronous machine. The results are relatively interesting.

To improve fault diagnosis, a second approach has been proposed. This method uses the same approach as described above, the only difference lies in the fact that this is not the phase of the Fourier transform of the Neutral Voltage which is analyzed by the program decision, but the phases of the analytic signal obtained by Hilbert transform of the amplitude spectrum of Neutral Voltage. This analysis helped to detect other defects that were not detected by the first approach.

In conclusion, the latest proposed method provides more meaningful results that the analysis of the phase spectrum of Neutral Voltage. Similarly, it would be interesting to validate this approach on asynchronous machines with different characteristics (higher power machines for example) to help determine a law of behavior for α parameter used in the detection criterion.

Appendix

TABLE IV WRIM Parameters

Parameter	***Value***	
Rated power	kW	3
Rated stator voltage	V	220
Rated frequency	Hz	50
Rated speed	rpm	1400
Stator phase resistance	Ω	0.621
Rotor phase resistance	Ω	0.4
Rotor inductance	H	0.013
Pole pairs		2

TABLE V WRIM Sensors

Parameter	***Value***	
Current sensor type		LA100
Current sensor accuracy	%	0.45
Current sensor Bandwidth	kHz	200
Voltage sensor type		DV1200
Voltage sensor accuracy	%	0.3
Voltage sensor Bandwidth	kHz	6.5

References

[1] F.Filippetti, A.Bellini and G.A. Capolino " Condition Monitoring and Diagnosis of Rotor Faults in Induction Machines: State of Art and Future Perspectives" *Electrical Machines Design Control and Diagnosis (WEMDCD), IEEE Workshop on pp. 196 – 209, 2013*

[2] A. Bellini, F. Filippetti, C. Tassoni, and G. Capolino, "Advances in diagnostic techniques for induction machines," *Industrial Electronics, IEEE Transactions on, vol. 55, no. 12, pp. 4109–4126, 2008.*

[3] Mohamed El Hachemi Benbouzid, "A Review of Induction Motors Signature Analysis as a Medium for Faults Detection" *IEEE Transactions on industrial electronics, vol. 47, no. 5, pp. 984-993 , october 2000*

[4] S. Nandi, H. Toliyat, and X. Li, "Condition monitoring and fault diagnosis of electrical motorsa review," *IEEE Transactions on Energy Conversion, vol. 20, no. 4, pp. 719–729, Dec. 2005.*

[5] P. Zhang, Y. Du, T. G. Habetler, and B. Lu, "A survey of condition monitoring and protection methods for medium-voltage induction motors," *IEEE Transactions on Industry Applications, vol. 47, no. 1, pp. 34–46, 2011.*

[6] Y. Gritli, L. Zarri, C. Rossi, F. Filippetti, G. Capolino, and D. Casadei, "Advanced diagnosis of electrical faults in wound rotor induction machines," *IEEE Transactions on Industrial Electronics, , p. 1, 2013.*

[7] J. H. Jung, J. J. Lee, and B. H. Kwon, "Online diagnosis of induction motors using MCSA," IEEE *Transactions on Industrial Electronics, vol. 53, no. 6, pp. 1842–1852, Dec. 2006.*

[8] A. Espinosa, J. Rosero, J. Cusido, L. Romeral, and J. Ortega, "Fault detection by means of hilbert-huang transform of the stator current in a pmsm with demagnetization," *Energy Conversion, IEEE Transactions on, vol. 25, no. 2, pp. 312 –318, june 2010.*

[9] G. Didier, E. Ternisien, O. Caspary, H. Razik "A new approach to detect broken rotor bars in induction machines by current

spectrum analysis" *Mechanical Systems and Signal Processing 21 pp. 1127–1142 , 2007*

[10] M. E. K. Oumaamar, H. Razik, A. Rezzoug, A. Khezzar "Line Current Analysis for Bearing Fault Detection Induction Motors Using Hilbert Transform Phase" *acemp, Electromotion 2011, pp. 289-294, 8-10 Sept 2011, Istanbul (Turkey).*

[11] Yuefeng Liao, Thomas A. Lipo , "Effect of saturation third harmonic on the performance of squirrel-cage induction machines" *Electric Machines & Power Systems, vol. 22, no2, pp. 155-171, 1994*

[12] M. A. Cash, T. G. Habetler, G. B. Kliman, "Insulation Failure Prediction in AC Machines Using Line-Neutral Voltages", in *IEEE Transactions on Industry Applications, Vol. 34, No 6, pp. 1234–1239,November/December 1998.*

[13] H. Razik and G. Didier, "A novel method of induction motor diagnosis using the line-neutral voltage," *in Proc. EPE-PEMC, Riga, Latvia, Sep. 2004.*

[14] M.E.K. OUMAAMAR « Surveillance et diagnostic des défauts rotoriques et mécaniques de la machine asynchrone avec alimentation équilibrée ou déséquilibrée » *PhD thesis (Groupe de Recherche en Electrotechnique et Electronique de Nancy GREEN-UdL Faculté des Sciences et Technologies) March 2012*

[15] Khezzar, A.; Oumaamar, M. E. K.; Hadjami, M.; Boucherma, M.; Razik, H.; "Induction Motor Diagnosis Using Line Neutral Voltage Signatures", *Industrial Electronics, IEEE Transactions on, Volume 56, Issue 11, Nov. 2009 Page(s):4581 – 4591.*

[16] M.E.K. Oumaamar, F. Babaa, A. Khezzar and M. Boucherma, "Diagnostics of Broken Rotor Bars in Induction Machines Using the Neutral Voltage", *ICEM'2006 Conference. Chania. Greece, 2- 5 September 2006.*

[17] M.E.K. Oumaamar, A. Khezzar, M. Boucherma, H. Razik, R. Andriamalala, L. Baghli, "Neutral Voltage Analysis for Broken Rotor Bars Detection in Induction Motors Using Hilbert Transform Phase" , *IAS 2007,43rd Annual meeting, New Orleans (USA),23-27 pp. 1940 - 1947 september.2007*

[18] J. Antonino-Daviu, M. Riera-Guasp, M. Pineda-Sanchez, and R. Perez, "A critical comparison between dwt and hilbert huang-based methods for the diagnosis of rotor bar failures in induction machines," Industry Applications, *IEEE Transactions on, vol. 45, no. 5, pp. 1794 –1803, sept.-oct. 2009.*

[19] Liru Han " Gear fault detection and diagnosis based on Hilbert-Huang transform" *Image and Signal Processing (CISP), 3rd International Congress on , Vol. 7 pp 3323 – 3326 , 2010*

Khalid Dahi was born in Errachidia, Morocco, in 1988. He received the M.S. degree in electrical engineering in 2012 from the Mohammed V Souissi University, Rabat-Morocco- where he is currently working toward the Ph.D. degree in the department of electrical engineering. Since 2012, His research interests are related to electrical machines and drives, diagnostics of induction motors. His current activities include monitoring and diagnosis of induction machines in wind motor.

Dr. Soumia El Hani, Professor at the ENSET (Ecole Normale Supérieure de l'Enseignement Technqique-Rabat, Morroco) since October 1992. Research Engineer at the Mohammed V Souissi University Morocco. In charge of the research team electromechanical, control and diagnosis. Member of the eesearch eaboratory in electrical engineering at ENSET -Rabat. In charge of electrotechnic and power electronic competences group. Author of several publications in the field of electrical engineering, including robust control systems, diagnosis and control systems of wind electric conversion.

Dr. Said GUEDIRA, Professeor at ENIM (Ecole Nationale de l'Industrie Minérale - Rabat – Morroco) since 1983. Research Engineer and Director of the research laboratory CPS2I (Control, protection et surveillance des installations industrielles). Author of several publications in the field of Electrical Engineering, including diagnosis and control of mechatronic systems.